Unusual Polarization Patterns in Flat Epitaxial Ferroelectric Nanoparticles

Ivan Naumov and Alexander M. Bratkovsky

Hewlett-Packard Laboratories, 1501 Page Mill Road, Palo Alto, California 94304, USA

(Received 20 June 2008; published 3 September 2008)

We investigate the effects of a lattice misfit strain on a ground state and polarization patterns in flat perovskite nanoparticles (nanoislands of $BaTiO_3$ and PZT) with the use of an *ab initio* derived effective Hamiltonian. We show that the strain strongly controls the balance between the depolarizing field and the polarization anizotropy in determining the equilibrium polarization patterns. Compressive strain favors 180° stripe or tweed domains while a tensile strain leads to in-plane vortex formation, with the unusual intermediate phase(s) where both ordering motifs coexist. The results may allow us to explain contradictions in recent experimental data for ferroelectric nanoparticles.

DOI: 10.1103/PhysRevLett.101.107601 PACS numbers: 77.80.Bh, 77.22.Ej, 77.84.Dy

Interest in epitaxial ferroelectric nanoislands is growing rapidly driven by their potential for nanodevices, especially ultradense memories [1–3]. Recent advances in the ''bottom-up'' (self-assembly) nanometer scale techniques have opened up the opportunities for fabricating high-quality epitaxial ferroelectric nanoislands with extremely small thickness and lateral size on the order of 1 nm and 20 nm, respectively [3–7]. On the other hand, recent emergence of powerful probes such as piezoresponse force microscopy (PFM) has enabled imaging of a local domain structure with sub-10 nm resolution [2,8,9]. In spite of those developments, a clear understanding of the origin of the polarization patterns in epitaxial ferroelectric nanoislands is still lacking. Here, we present the results of *ab initio* studies of nonelectroded epitaxial $Pb(Zr_{0.5}Ti_{0.5})O_3$ (PZT) and $BaTiO_3$ (BTO) nanoislands and find the existence of novel polarization patterns driven by the shape or depolarizing field, misfit strains, and/or anisotropy energy.

Geometrically, nanoislands or flat ferroelectric (FE) nanoparticles is a class of systems bridging the gap between 0D nanodots and 2D ultrathin films. Compared with thin films, they have free-standing sidewalls that tend to suppress the formation of a nonuniform in-plane polarization because of appearing depolarizing field, similar to the ferromagnetic particles [10]. On the other hand, relative to the (confined in all three dimensions) nanodots, they have large aspect ratio and likely to behave similarly to thin films when the polarization is out of plane. These observations lead one to expect that ferroelectric nanoislands should exhibit some kind of a ''particle-to-thin film'' crossover behavior and related novel effects depending on the aspect ratio and the type of bulk polarization ordering (which is different in PZT compared to BTO crystals).

Free-standing perovskite ferroelectric nanodots usually lose stability with respect to a vortex ground state, where the polarization curls around some vortex core(s). Such an ordering can be characterized, in a simplest single vortex case, by a *toroidal* moment or a moment of polarization [11,12]. On the other hand, the epitaxial perovskite thin films typically become uniaxial under compressive strain with an easy axis perpendicular to the film, and usually form a 180° stripe (c-)domain structure [13–18]. One can, therefore, anticipate the flat ferroelectric nanoislands with large aspect ratio to undergo an unusual vortex to stripe domains transformation with an increasing compressive misfit strain. We show below that perovskite nanoislands do indeed undergo such a transition, but only via one or two *intermediate* phases where in-plane curling polarization coexists with the 180° c domains. Moreover, the domain phase does not necessarily render the well-known 180° stripe domain structure, but can take a form of a 180° *tweed texture*.

The simulated nanoparticles have circular and/or rectangular shapes and the following dimensions: 19×6, 39×10 for the disks and $39 \times 39 \times 10$ for the square particles (all dimensions are given in lattice parameters of the cubic bulk phase a, which is 4.00 Å and 3.95 Å for PZT and BTO, respectively.) The z axis is selected along the (shortest) pseudocubic [001] direction normal to the substrate. To simulate finite-temperature behavior of the particles, we use the effective Hamiltonian

$$H = H(\{\boldsymbol{u}_i\}, \{\boldsymbol{v}_i\}, \{\sigma_i\}, \{\boldsymbol{\epsilon}\}), \tag{1}$$

which is a function of the local modes $\boldsymbol{u}_i$ (proportional to the local dipoles $\boldsymbol{p}_i$), the inhomogeneous strain $\boldsymbol{v}_i$, and alloy species σ_i at site i, as well as the homogenous strain $\boldsymbol{\epsilon}$ [19,20]. The first-principles derived parameters for bulk BTO are given in Ref. [19], and for a bulk PZT in Ref. [20]. In addition to the bulk terms, the Hamiltonian also contains the corrections associated with the presence of free surface: ''vacuum-local mode'' and ''vacuum-inhomogeneous strain'' interactions [21,22]. Typically, 40 000 Monte Carlo sweeps have been used to find the equilibrium dipole configuration at a fixed temperature. Open-circuit boundary conditions are assumed, so that no screening charges are taken into consideration. The effect of a substrate is imposed by fixing the homogeneous in-plane strain in the whole island: $\epsilon_{xx} = \epsilon_{yy} = \epsilon$, $\epsilon_{xy} = 0$.

Our calculations predict that at low temperatures all the investigated *unstrained* nanoparticles transform into a vortex ground state characterized by a nonzero toroidal moment $\boldsymbol{G} = (2N)^{-1}\sum_i \boldsymbol{r}_i \times \boldsymbol{p}_i$, where N is the total number of unit cells. In the disk-shaped PZT particles [Figs. 1(a) and 1(b)], the local dipoles rotate from cell to cell forming the classical vortex patterns. On the other hand, in a rectangular PZT $39 \times 39 \times 10$ particle the polarization aligns with the square boundary as much as possible, hence the discontinuity lines (domain walls) form, and the resulting pattern can be viewed as four closure domains separated by 90° domain walls [Fig. 1(c)]. The polarization in each domain points along one of the four pseudocubic $[\pm 100]$ and $[0 \pm 10]$ directions, so that the domain walls are parallel to the (1 ± 10) crystallographic planes and pass through the center of the particle. In BTO particles, regardless of their shape and size, the dipoles tend to be along the $[\pm 1 \pm 10]$ directions [Figs. 1(d)–1(f)]. As a result, two (100)-type 90° domain walls are likely to be formed crossing each other at the geometric center of the particles. The walls are rather fuzzy in bigger particles, especially in a rectangular $39 \times 39 \times 10$ dot where the dipoles are frustrated near the lateral surfaces.

The different behavior of PZT and BTO unstrained nanoparticles can be easily understood by inspecting their bulk limits. PZT in the bulk form adopts a tetragonal structure with an "easy" direction of polarization along [100]. At the same time, bulk BTO has a rhombohedral equilibrium structure with the easy direction along [111]. Let us compare now, for example, the two $39 \times 39 \times 10$ PZT and BTO particles. In both cases, the effects of depolarizing field force the dipoles to lie in the x-y plane. In the case of the PZT particle, however, the materials anisotropy factor is in compliance with the shape: majority of the dipoles are oriented along the easy directions [100] and [010] and at the same time they are parallel to the surface. The situation is quite different for the BTO particles, where *none* of the dipoles can be directed along the easy [111] body diagonal: in this case the majority of dipoles in the center region prefers to be oriented along [110] instead of the [111] direction. Near the side walls, however, the depolarizing field forces the dipoles to align with the square geometry, which increases the anisotropy energy term. The competition between those forces leads to the dipole frustration near the vertical walls and to the formation of four additional vortices near the corners [Fig. 1(f)] in agreement with the previous calculations for a $24 \times 24 \times 24$ BTO nanodot [21].

The tensile strains stabilize the vortex states, as seen from Fig. 2, increasing the z component of the toroidal moment. On the contrary, compressive strains enhance the out-of-plane polarization, decrease G_z and eventually lead to a 180° multidomain structure running through the entire thickness of the islands (see below). It is remarkable that in the case of BTO particles the critical strain associated with this transition is very small, close to zero, $\approx 0\%$. In the PZT case, the critical strain dramatically decreases from 1.2% to $\approx 0\%$ when one increases the particle diameter from 19 to 39. The bigger PZT particle in a vortex state can tolerate the compressive strains less because its optimal in-plane averaged lattice parameter is noticeably larger than that corresponding to the bulk cubic phase [Fig. 2(b)].

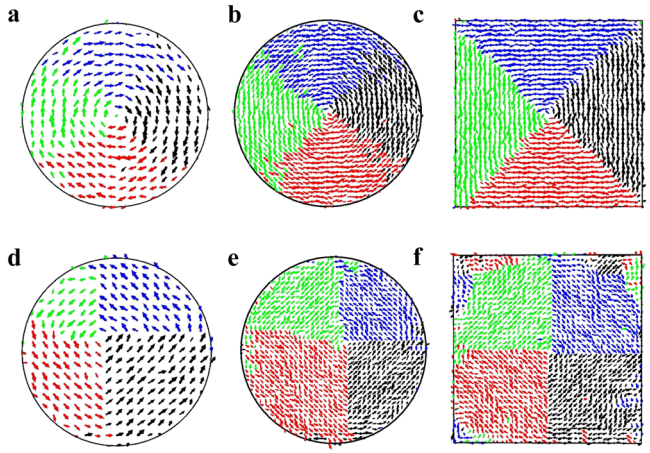

FIG. 1 (color online). Low-temperature polarization distributions on the central z plane in PZT (a)–(c) and BTO (d)–(f) nanoparticles in unstrained states. (a),(d)- 19×6 nanodisks, (b), (e)- 39×10 nanodisks and (c),(f)- $39 \times 39 \times 10$ particles with square footprints. Shown in red, blue, green, and black are the dipoles directed predominantly along $[\pm 100]$ and $[0 \pm 10]$ in PZT and along $[\pm 1 \pm 10]$ in BTO systems.

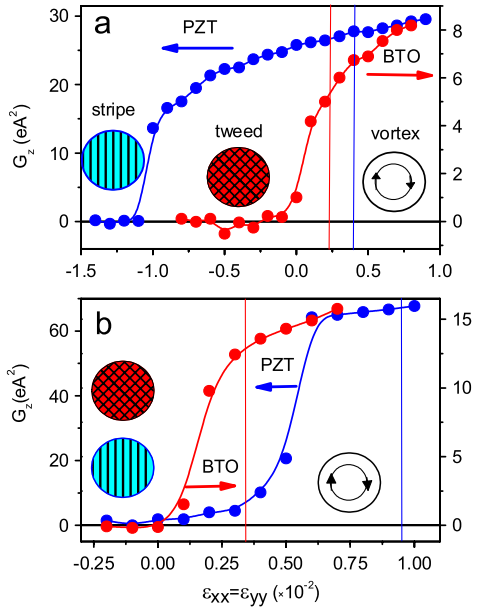

FIG. 2 (color online). The z component of the toroidal moment as a function of strain in 19×6 (a) and 39×10 (b) nanoparticles. The strains are measured relative to the LDA-calculated lattice constants in bulk cubic structures. Note that in free-standing states the particles are characterized by the nonzero "residual" strains marked by vertical lines. The residual strain increases in 39×10 compared to 19×6 particle, especially in PZT.

In the PZT nanoparticles, the 180° multidomain phase is nothing but the well-known 180° stripe domain structure calculated previously in infinite PZT thin films [17]. Here, like in the thin films, the "up" and "down" domains run along [100] and alternate along [010] direction [Fig. 3(a) and 3(b)]. The domain width, however, is not homogeneous across the particles: it is larger in the interior region and becomes 1–2 unit cell narrower near the edge of the particles. Besides, the stripes become wider in bigger particles. In a circular 19×6 particle, for example, the width of the central stripe is 4 unit cells (16 Å), while it is 6 unit cells wide (24 Å) in 39×10 and $39 \times 39 \times 10$ particles. In both cases, the stripes are narrower than the 8 unit cells thick domains found in twice thinner PZT thin films (5 unit cells thick) [17]. One would have expected that the domain width in the twice thicker particles would be $\sqrt{2}$ larger if the Landau "square root" law for domain width versus film thickness [13] were to apply to the flat nanoparticles. However, we see that this is not the case, indicating possible large deviations from the law.

BTO nanoparticles, in comparison with PZT counterparts, adopt not straight but curved zigzag type stripes, running predominantly in [110] and $[1\bar{1}0]$ directions [Figs. 3(c) and 3(d)]. Though rarely, they intersect each other forming a 180° tweed domain texture, which is drastically different from the stripe domain structure found in BTO thin films [14,18]. In the case of thin films, the stripes run only along one direction (either [110] or $[1\bar{1}0]$) and the system loses its fourfold symmetry axis perpendicular to the film. In the nanoparticles, however, the axis of the 4th order is (on average) preserved by stripes propagating in both possible directions. The stripes width changes from place to place, being less than 4 lattice constants on average. This value can be compared with 4.3 lattice periods found in BTO thin films [18] modeled with $24 \times 24 \times 5$ supercell. This relation between the domain widths is analogous to the above discussed case of the PZT particles.

As the present analysis shows, the transformation "vortex-to-180° domains" does not occur directly, but rather via one or even two intermediate structures. The simplest case is presented by a 19×6 PZT particle having only a single intermediate structure. This structure develops from the vortex core that turns out to be longitudinally polarized already in a free-standing state. While the core region (with the radius of 3-4 lattice spacings) has the polarization pointing "up", beyond this radius the polarization tilts slightly out of plane oppositely to the core region, so that all the dipoles add up to zero (Fig. 4). Under compressive strain, the vortex core radius expands and becomes comparable to the lateral size of the particles. At this stage, the x, y components of the local dipoles still form a vortex, while the out-of-plain component, z, breaks the system into coaxial oppositely polarized cylindrically symmetric domains, in other words, a Skyrmion-like structure [23]. As the compressive strain further increases, this structure abruptly transforms into a 180° stripe domain phase with zero toroidal moment $\boldsymbol{G}$ [Fig. 2(a)].

In all other particles (both PZT and BTO), the structural transformation into 180° domain phase occurs in a two-step fashion. At first and relatively short stage, again, two symmetry conforming 180° coaxial domains develop at the expense of the toroidal moment forming a Skyrmion structure. As the in-plane compression increases, this Skyrmion structure transforms into 180° stripe (tweed) domains on the background of *nonzero* G_z. And, finally, the toroidal moment disappears at a critical compressive

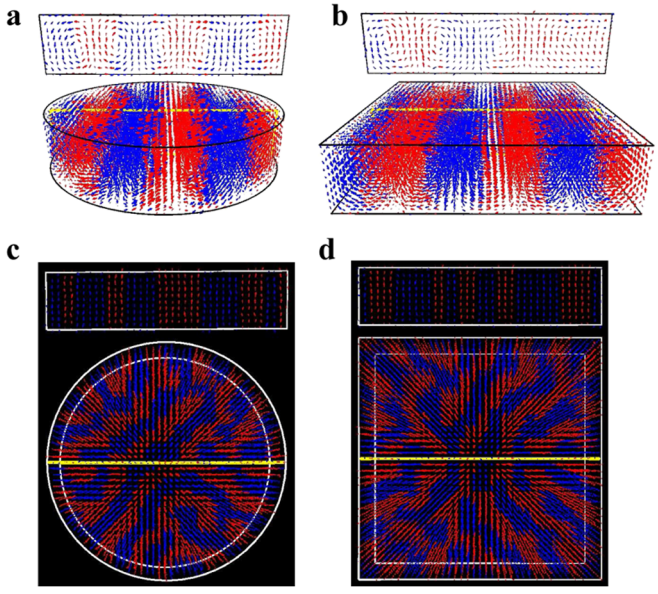

FIG. 3 (color online). Low-temperature three-dimensional polarization patterns in the free-standing (001) PZT (a),(b) and BTO (c),(d) nanoparticles under compressive strain of −2%. (a), (c)- 39×10 nanodisks, (b),(d)- $39 \times 39 \times 10$ particles with square footprints. The small rectangular insets show the cross sections of a central vertical plane marked by the yellow lines. The red and blue arrows show local dipoles with positive and negative z component, respectively.

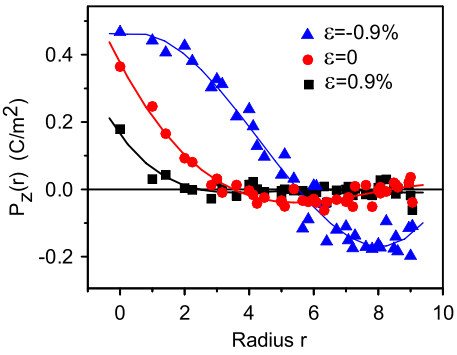

FIG. 4 (color online). Vertical polarization component in the 19×6 PZT disk at different misfit strains. While the values are radially averaged, they correspond to an instant moment of time and represent the fluctuating dipole structure. The lines represent 4th order polynomial fits to the instant polarizations.

strain, and the system enters into a pure stripe or tweed domain phase.

All the considered above intermediate phases (including Skyrmion-like) are characterized by z domains coexisting with the in-plane curling polarization; they can be called the ''domain-patterned vortex'' structures. Interestingly, such structures have never been reported for ferroelectric small systems, although have been found in flat magnetic particles with low perpendicular anisotropy [24]. Analogously, the 180° tweed domain texture [Figs. 3(c) and 3(d)] has never been discovered in ferroelectric nanostructures, although it pretty much resembles the labyrinthine phase observed in ultrathin magnetic films [25]. One can think that this relatively high-symmetric structure is due to in-plane isotropic compression and will evolve into an ordinary stripe phase if the symmetry is broken by making strain slightly anisotropic. We checked this assumption by adding pure shear components $(\epsilon_{xx} - \epsilon_{yy})/2$ and ϵ_{xy} to the initially homogeneous in-plane compressive strain ϵ and found the tweed structure to be robust against the additional distortions as large as 2% for very long computer simulations (500 000 MC sweeps).

Our predictions can be helpful for understanding some puzzling and controversial experimental results [4–7]. While the authors [4,6] did not observe any piezoresponse of the $PbTiO_3$ islands with the diameters smaller than 20 nm, Ref. [5] reported observation of ferroelectricity in zirconate titanate nanoparticles with the lateral size as small as 9 nm. On the other hand, according to measurements [7], the relationship between the size of nanoislands and occurrence of ferroelectricity is rather random, raising the question why some particles are ferroelectric, but others (even with very similar sizes) are not. Based on our results, we can explain the discrepancies in the experimental results in the following way. As compared with continuous thin films, the existence of free side walls in nanoislands leads to new and additional mechanisms of the strain relaxations [26], including formation of partial or full misfit dislocations at nodes of the lateral surfaces and the flat plane of the substrate. This implies that with decreasing lateral size the maintaining coherent mismatch lattice strains in a nanoisland becomes more and more difficult, and it is very likely that under the same experimental conditions the smaller particles will experience less external strain. Moreover, since the magnitude of the strain is not well controlled, even the particles with comparable sizes can be differently strained. But in this case, according to our calculations, they can show totally different piezoresponses. Indeed, as the compressive strain is relaxed, an island can transform into an intermediate or even in a vortex state, which is unable to produce any (vertical or lateral) PFM signal at all. The particle in a vortex state should be viewed as a paraelectric one exhibiting only linear and hysteresis-free piezoresponse as a function of dc bias voltage applied to the AFM tip, conforming to some observations.

In summary, we have investigated the strain effects on (001)-epitaxial PZT and BTO nanoislands using first-principles-derived effective Hamiltonian approach. Our study leads to the following conclusions: (i) regardless of a size, shape, and a type of a perovskite material, all the investigated *unstrained* flat nanoparticles transform into a vortex state with an in-plane curling polarization, (ii) under strong enough compressive strain the vortex state is no longer stable and gives way to a 180° stripe domain phase in PZT and to a more symmetric, 180° tweed domain texture, in BTO nanoparticles, and (iii) these transitions proceed via one or two *unusual* intermediate phases where a 180° domain structure coexist with circular in-plane vortex ordering. The obtained results seem to resolve controversies observed in recent data.

[1] J. F. Scott, Science **315**, 954 (2007).
[2] A. Gruverman and A. Kholkin, Rep. Prog. Phys. **69**, 2443 (2006).
[3] M. Alexe and D. Hesse, J. Mater. Sci. **41**, 1 (2006).
[4] A. Roelofs *et al.*, Nanotechnology **14**, 250 (2003).
[5] K. S. Seol, K. Takeuchi, and Y. Ohki, Appl. Phys. Lett. **85**, 2325 (2004).
[6] M. Okaniwa *et al.*, Jpn. J. Appl. Phys. **44**, 6891 (2005).
[7] M. Shimizu *et al.*, in Abstracts of the International Symposium on Integrated Ferroelectrics (ISIF 2006), 4-380-C , Honolulu, Hawaii, USA, April 23-27, 2006.
[8] *Nanoscale Characterisation of Ferroelectric Materials: Scanning Probe Microscopy*, edited by M. Alexe and A. Gruverman (Springer, Berlin, 2004).
[9] A. R. Rüdiger *et al.*, Appl. Phys. Lett. **80**, 1247 (2005).
[10] A. Hubert and R. Schäfer, *Magnetic Domains* (Springer, Berlin, 1998).
[11] I. Naumov, L. Bellaiche, and H. Fu, Nature (London) **432**, 737 (2004).
[12] I. Ponomareva *et al.*, Phys. Rev. B **72**, 140102(R) (2005).
[13] A. M. Bratkovsky and A. P. Levanyuk, Phys. Rev. Lett. **84**, 3177 (2000).
[14] S. Tinte and M. G. Stachiotti, Phys. Rev. B **64**, 235403 (2001).
[15] S. K. Streiffer *et al.*, Phys. Rev. Lett. **89**, 067601 (2002).
[16] D. D. Fong *et al.*, Science **304**, 1650 (2004); Phys. Rev. B **71**, 144112 (2005).
[17] B.-K. Lai *et al.*, Phys. Rev. Lett. **96**, 137602 (2006).
[18] B.-K. Lai *et al.*, Phys. Rev. B **75**, 085412 (2007).
[19] W. Zhong, D. Vanderbilt, and K. M. Rabe, Phys. Rev. B **52**, 6301 (1995).
[20] L. Bellaiche, A. Garcia, and D. Vanderbilt, Phys. Rev. Lett. **84**, 5427 (2000); Ferroelectrics **266**, 41 (2002).
[21] H. Fu and L. Bellaiche, Phys. Rev. Lett. **91**, 257601 (2003).
[22] E. Almahmoud *et al.*, Phys. Rev. B **70**, 220102(R) (2004).
[23] U. K. Röler, A. N. Bogdanov, and C. Pfleiderer, Nature (London) **442**, 797 (2006).
[24] A. Maziewski, V. Zablotskii, and M. Kisielewski, Phys. Rev. B **73**, 134415 (2006).
[25] O. Portmann, A. Vaterlaus, and D. Pescla, Nature (London) **422**, 701 (2003).
[26] I. A. Ovid'ko, Phys. Rev. Lett. **88**, 046103 (2002).